

Andrographolide Ameliorates Inflammation through Inhibition of NLRP3 Inflammasome Activation in Intestinal Epithelial Cells

Khanna K¹, Mishra KP^{2*}, Ganju L¹, Kumar B¹ and Singh SB³

¹Defence Institute of Physiology and Allied Sciences (DIPAS, DRDO) Delhi, India

²Defence Research and Development Organisation (DRDO), New Delhi, India

³National Institute of Pharmaceutical Education and Research (NIPER), Hyderabad, India

Received: 04 Nov 2019

Accepted: 21 Nov 2019

Published: 29 Nov 2019

*Corresponding to:

Kamla Prasad Mishra, Defense Research and Development Organisation, New Delhi, India, Tel: +91 11 23007342, Email: kpmppi@rediffmail.com

1. Abstract

Stressors have varied biological effects on gastrointestinal system which are increasingly recognized as enhanced gut permeability, dysbiosis and inflammation in the gut. Endotoxins, the metabolites released by harmful gut microbes are one of the stressors resulting in these problems. Hypobaric hypoxia, being another harmful stressor for the gut, requires the discovery of some prompt treatments. Andrographolide is a major bioactive component of traditional medicinal plant *Andrographis paniculata* which shows anti-inflammatory effects in different organs. Compared to its anti-inflammatory effect on vital organs, its effect on intestine is mostly untried. In our study, we investigated the impact of andrographolide in acute models of intestinal injury and studied the molecular mechanisms of andrographolide in modifying stress-induced signaling pathways. Andrographolide treatment in intestinal epithelial cells (IEC-6) was found to reduce nitric oxide, a key signaling molecule in the pathogenesis of inflammation, in LPS induced cells. Andrographolide treatment suppressed the levels of proinflammatory cytokines and inflammasome activation by downregulating NLRP3, caspase-1. Also, hypobaric hypoxia being the cause of intestinal barrier injury and inflammation results in an increase of endotoxin translocation to the intestine. In hypobaric hypoxia (HH) induced rat model, andrographolide was seen to suppress proinflammatory cytokines and intestinal inflammation via NLRP3 pathway. These results suggest that andrographolide could be a potential drug candidate for the treatment of intestinal inflammation-related problems.

2. Keywords: Inflammasome; Intestinal epithelial cells; Proinflammatory cytokines; LPS; Andrographolide

3. Introduction

Herbal medicines are the main source of treatment for about 80 % world's population, majorly in the developing countries due to better compatibility in the human body with lesser side effects [1]. The *Andrographis paniculata*, generally known as "King of bitters" is a plant traditionally used in Asian medicine. *Andrographis paniculata* (Burm. F) Neesarean herbaceous plant of the

family Acanthaceae and has been used to treat flu, sore throat and upper respiratory tract infections in different regions of Asia [2]. Andrographolide, a major bioactive constituent of the plant extracted from its leaves has been known to show many pharmacological properties like antibacterial, antiviral, anti-tumor, anti-inflammatory, anti-cancer, anti-diabetic, immunomodulatory, etc [3,4].

Intestinal epithelial cells function as a physical barrier

to separate lumen from underlying lamina propria and intestinal layers. LPS, an endotoxin presents as a major cell wall component in gram-negative bacteria concentrates majorly in the gut lumen due to the presence of commensal bacteria residing there. In a healthy body, LPS cannot penetrate across intestinal epithelium barrier while increased intestinal permeability as in case of IBD, NEC & other bacterial or viral stresses can exaggerate paracellular flux of LPS and hence can cause intestinal inflammation [5]. Further, research studies have also shown hypobaric hypoxia (HH) as a stress factor to cause intestinal barrier injury, thus leading the translocation of endotoxins and intraluminal bacteria across the barrier which can cause inflammation and multiple organ failure [6].

Nitric oxide (NO) is a signaling molecule in the pathogenesis of inflammatory conditions and thereby considered as pro-inflammatory mediator to induce inflammation by its over production [7]. Dysregulation of mucosal immunity results in overproduction of pro-inflammatory cytokines which causes uncontrolled intestinal inflammation [8]. Suppression of these cytokines may help in regulating the inflammation at the gut mucosal levels. Also, NLRP3 inflammasome is known to activate host immune responses on sensing disturbances in cellular homeostasis [14]. Inflammasome assembly triggers the conversion of procaspase-1 to active caspase-1 which further converts pro IL-1 β to biologically active IL-1 β [9]. Previous studies have shown activation of inflammasome on LPS treatment and new treatment strategies are being developed for its suppression using different interventions in different organs [10,11]. On the other hand, heat shock proteins (HSPs) also known as stress proteins play a major role in protecting cells against stress/apoptosis [12]. HSPs show cytoprotective functions by preventing the aggregation of denatured proteins, initiating their refolding or proteolytic degradation [13].

In our study, andrographolide potentially lowers nitric oxide levels and expression of Heat Shock Proteins (HSPs) in LPS induced intestinal epithelial cells. Andrographolide has also shown to potentially inhibit activation of NLRP3 inflammasome in LPS and HH induced stress conditions. Our study offers a mechanistic basis for the therapeutic potential of andrographolide in

sepsis and other inflammatory diseases.

4. Material and Methods

4.1. Cell Culture and Treatment

The non-transformed rat intestinal epithelial cell lines (IEC-6) were obtained from National centre for cell science (NCCS, Pune, India) and maintained in DMEM high glucose (Himedia, India, AL111) supplemented with 10 % fetal bovine serum (Sigma, USA, F4135) at 37 °C, 5 % CO₂. Commercially available LPS (Sigma, USA, L2654) was prepared in 1 mL sterile PBS (Phosphate buffered saline, pH 7.4) to get a final concentration of 1 mg/mL. Reconstituted LPS was diluted further to working concentrations (1, 2.5 and 5 μ g/mL) using PBS. Stock solution (5 mg/ml) of andrographolide (Sigma, USA, 365645) was prepared in 1 % DMSO in PBS. Further working concentrations of andrographolide (1 μ g/mL and 10 μ g/mL) were made in PBS.

4.2. Cell Viability Assay

IEC-6 cells at a concentration of 1 x 10⁶ cells/mL were treated with 1, 2.5 and 5 μ g/mL doses of LPS for 48 h. 3-(4,5-dimethyl-2-thiazolyl)-2,5-diphenyltetrazolium bromide (MTT) (Sigma) dye was prepared in PBS at stock concentration of 5 mg/mL concentration. 10 μ l of MTT stock was added to cultured cells and incubated for 4 h at 37 °C. Viable cells reduced MTT to dark-blue colored formazan crystals. Crystals were then dissolved by the addition of dimethyl sulphoxide (DMSO). Optical density was measured at 570 nm using spectrophotometer (BioTek Instruments, USA). Readings were used to calculate % viable cells on LPS treatment. Upon LPS dose standardization, cell viability at 1 μ g/mL and 10 μ g/mL doses of andrographolide was checked using MTT.

4.3. Nitric Oxide Estimation

IEC-6 cells at concentration 1 x 10⁶ cells/mL were cultured and treated as per groups i.e. LPS (2.5 μ g/mL), andrographolide (1 μ g/mL), LPS (2.5 μ g/mL) along with andrographolide (1 μ g/mL) and control cells (without treatment). After 48 h, supernatant from different samples was collected and the indirect assay was performed by measuring nitrite, a by-product of NO biodegradation. Griess reagent (equal volumes of N-(1-naphthyl) ethylenediamine and sulfanilic acid) was added to samples to form pink color on nitrite detection.

Absorbance was taken at 540 nm using spectrophotometer (Biox-Tek Instruments, USA). A standard curve was formed using different serial dilutions of nitrite standard solution (NaNO_2) to estimate nitric oxide concentration in the samples.

4.5. Hypobaric Hypoxia and Dosing

Male Sprague-Dawley rats bred in IEAC (Institutional Ethical Committee on Animal Experimentations) approved animal facility of DIPAS (Defence Institute of Physiology and Allied Sciences), Delhi, India [Approval number: DIPAS/IAEC/2017/07], weighing 200 ± 20 g were given andrographolide orally by gavage method at a dose of 20 mg/kg/BW starting 3 days prior to acclimatization of HH exposure at 15000 ft and continuing to 7 days of HH exposure of 25000 ft (282 torr pressure) in animal decompression chamber. Animals were fed with rodent pellet and water ad libitum at 25 ± 1 °C, 55 ± 10 % humidity. The animal decompression chamber was opened for 15 min/day for the replenishment of water, food, bedding and cage. A continuous supply of fresh air at a rate of 8 L/min was provided to prevent carbon dioxide accumulation. Animals of normoxia groups were kept in the same environment without hypoxia exposure. After completion of the exposure, animals were euthanized by giving an overdose of sodium thiopental (90 mg/Kg). Experiments were performed in strict compliance with guidelines of 'Committee for the Purpose of Control and Supervision of Experiments on Animals' (CPCSEA), Government of India.

4.6. Haematoxylin and Eosin (H&E) Staining

Immediately after the completion of 7 days of HH exposure, rats were sacrificed and jejunum tissue was collected in 10 % formalin solution. Paraffin embedding and staining were done as explained by Khanna et al. 2018.

4.7. Sample Preparation

IEC-6 cells at 4 million/mL concentration, untreated, LPS treated (2.5 $\mu\text{g}/\text{mL}$), andrographolide treated (1 $\mu\text{g}/\text{mL}$) and LPS (2.5 $\mu\text{g}/\text{mL}$) with andrographolide (1 $\mu\text{g}/\text{mL}$) treated, were cultured in six-well plate (2 mL per plate) for 48 hrs. The cells were collected and washed twice with ice-cold PBS. The whole cell lysate was prepared at 10,000 Xg for 20 min in whole cell lysis buffer (0.1M HEPES, 0.5M EDTA, 0.1M EGTA, 2M KCl, 5M NaCl, 0.1M DTT,

protease inhibitor cocktail, Triton-X 100). Total protein concentration was estimated using the Bradford method. Whole cell lysate preparation from jejunum tissue stored immediately at -80 °C post-sacrifice was prepared with the same protocol.

4.8. Immunoblot Analysis

10 % separating and 5 % stacking gels were prepared. Samples were loaded; electrophoresis at 80 V was initiated and changed to 120 V after 30 min until samples run to the bottom. Proteins were then transferred to PVDF membrane (Millipore) in a semi-dry transfer blot system (Bio-rad). The resulting membrane was blocked with 5 % BSA in TBS for 1 h. Primary antibody anti-HSP-60 (1:1000, Santa Cruz Biotechnology, USA, sc-13115 {secondary: anti-mouse HRP}), anti-HSP-70 (1:1000, Santa Cruz Biotechnology, USA, sc-24 {secondary: anti-mouse HRP}), anti-Caspase-1 (1:1000, St. John's labs, UK, STJ92017 {secondary: anti-Rabbit HRP}), anti-NLRP3 (1:1000, St. John's labs, UK, STJ27619 {secondary: anti-rabbit HRP}) and anti- β -actin-HRP labelled (1:1000, Abcam, UK, ab8226 {secondary: anti-mouse HRP}) were added at 4 °C overnight. Subsequently, the membrane was washed with TBST (TBS with 0.01 % Tween-20) thrice for 5 min. A secondary antibody (Anti-rabbit HRP {1:10000, Abcam, UK, ab7621} and anti-mouse HRP {1:10000, Abcam, UK, ab97046}) was added for 1 h at room temperature and the membrane was again washed with TBST thrice for 10 min. Blots were developed and analyzed using ImageJ software.

5. ELISA

The supernatant was collected from all 4 different groups. Rat ELISA kits, TNF- α (PeproTech, USA, 900-K73), IL-1 β (PeproTech, USA, 900-K91) and IL-6 (PeproTech, USA, 900-K86) were used to estimate their levels in cell supernatant and gut lavage (gut lavage collection protocol as described by Khanna et al. 2018). ELISA plate (Greiner) was taken and coated with capture antibody overnight at 4 °C. Next day, after washing with wash buffer i.e. PBST (PBS with 0.1 % Tween-20), blocking buffer (1 % BSA in PBST) was added for 2 h at 37 °C. After washing, serial dilutions of standard provided in kit along with samples were added and incubated for 2 h at 37 °C. Biotin labelled secondary antibody was added in plate and incubation was done at 37 °C. After wash with PBST, streptavidin HRP conjugated solution was added.

TMB substrate solution provided in the kit was added for color development. The concentration of all cytokines in samples was estimated by plotting a standard curve using curve expert 1.4 and graph along with statistical analysis was plotted using Graph-Pad Prism software.

6. Statistical Analysis

Data were presented as mean \pm SEM. Difference between mean values of normally distributed data was analyzed using one-way ANOVA. The criteria for differences were considered significant below $p < 0.05$ in all experiments.

7. Results

7.1. Cell Viability at Different Concentration of LPS and Andrographolide on IEC-6 Cells

LPS at different doses of 1 $\mu\text{g}/\text{mL}$, 2.5 $\mu\text{g}/\text{mL}$ and 5 $\mu\text{g}/\text{mL}$ were given to rat intestinal epithelial cells (IEC-6) for 48 h and cell viability was assayed using MTT. LPS at a dose of 2.5 $\mu\text{g}/\text{mL}$ showed maximum % cell viability and minimum toxicity, thus used for further experiments in the study (**Figure 1A**). The mean \pm SEM of % cell viability at dose of 1 $\mu\text{g}/\text{mL}$, 2.5 $\mu\text{g}/\text{mL}$ and 5 $\mu\text{g}/\text{mL}$ was found to be 105.5 \pm 1.45 %, 115.1 \pm 2.13 % and 94.53 \pm 10.87 % respectively. Six groups i.e., Control (untreated), LPS (2.5 $\mu\text{g}/\text{mL}$), Andrographolide (1 $\mu\text{g}/\text{mL}$ and 10 $\mu\text{g}/\text{mL}$), LPS (2.5 $\mu\text{g}/\text{mL}$) along with andrographolide (1 $\mu\text{g}/\text{mL}$) and LPS (2.5 $\mu\text{g}/\text{mL}$) along with andrographolide (10 $\mu\text{g}/\text{mL}$) were further checked for % cell viability. The mean \pm SEM of % cell viability at different doses were 101.5 \pm 0.53 %, 105.6 \pm 0.58 %, 26.42 \pm 3.58 %, 105.4 \pm 0.37 % and 29.80 \pm 3.2 % when compared to control group. Andrographolide at dose 10 $\mu\text{g}/\text{mL}$ was found to be viable in less than 30% of the cells and hence andrographolide at 1 $\mu\text{g}/\text{mL}$ was taken for further experiments (**Figure 1B**).

7.2. Andrographolide Decreased Nitric Oxide Levels in LPS Treated IEC-Cells

Nitric oxide plays an important mediator in inflammatory responses. LPS was found to increase nitric oxide ($p < 0.01$) measured indirectly in terms of nitrite (μM) in intestinal epithelial cells while andrographolide decreased nitrite levels in LPS induced cells ($p < 0.05$) (Fig 1C). Nitrite levels at control, LPS (2.5 $\mu\text{g}/\text{mL}$), Andrographolide (1 $\mu\text{g}/\text{mL}$) and LPS (2.5 $\mu\text{g}/\text{mL}$) along with andrographolide (1 $\mu\text{g}/\text{mL}$) were found to be 10.60 \pm 0.30 μM , 15.36 \pm 1.17

μM , 7.57 \pm 0.03 μM and 11.79 \pm 0.60 μM respectively.

7.3. Andrographolide Downregulated Pro-Inflammatory Cytokines (TNF- α , IL-1 β , IL-6) and Expression of Heat Shock Proteins (HSP60, HSP70) in LPS Induced Intestinal Cells

Dysregulation of mucosal immunity was estimated by checking the levels of pro-inflammatory cytokines i.e. TNF- α , IL-1 β , IL-6 using ELISA. Levels of TNF- α (**Figure 2A**) in control was 0.1 \pm 0.01 pg/ml whereas LPS (2.5 $\mu\text{g}/\text{mL}$), Andrographolide (1 $\mu\text{g}/\text{mL}$) and LPS (2.5 $\mu\text{g}/\text{mL}$) along with andrographolide (1 $\mu\text{g}/\text{mL}$) groups had 0.19 \pm 0.02 pg/ml, 0.09 \pm 0.01 pg/ml and 0.10 \pm 0.01 pg/ml respectively ($p < 0.01$ in control vs LPS, LPS vs andrographolide and LPS vs LPS along with andrographolide). IL-1 β levels (**Figure 2B**) were found to be 0.12 \pm 0.01 pg/ml, 0.23 \pm 0.06 pg/ml, 0.10 \pm 0.01 pg/ml and 0.15 \pm 0.03 pg/ml in control rats, LPS (2.5 $\mu\text{g}/\text{mL}$), Andrographolide (1 $\mu\text{g}/\text{mL}$) and LPS (2.5 $\mu\text{g}/\text{mL}$) along with andrographolide (1 $\mu\text{g}/\text{mL}$) groups respectively. Levels of IL-6 (**Figure 2C**) in control was 1.77 \pm 0.31 ng/ml whereas LPS (2.5 $\mu\text{g}/\text{mL}$), Andrographolide (1 $\mu\text{g}/\text{mL}$) and LPS (2.5 $\mu\text{g}/\text{mL}$) along with andrographolide (1 $\mu\text{g}/\text{mL}$) groups had 2.60 \pm 0.24 ng/ml, 1.31 \pm 0.19 ng/ml and 0.39 \pm 0.19 ng/ml respectively ($p < 0.05$ in LPS vs andrographolide and LPS vs LPS along with andrographolide). Heat shock proteins like HSP-60 and HSP-70 are activated in response to any stress and are responsible for protein folding. Expression of HSP-60 has been found to decrease with andrographolide treatment following LPS infection (**Figure 2D, 2E**). Mean \pm SEM of densitometry for HSP-60 protein were 0.43 \pm 0.19, 0.70 \pm 0.36, 0.27 \pm 0.09, 0.24 \pm 0.067 in control, LPS (2.5 $\mu\text{g}/\text{mL}$), Andrographolide (1 $\mu\text{g}/\text{mL}$) and LPS (2.5 $\mu\text{g}/\text{mL}$) along with andrographolide (1 $\mu\text{g}/\text{mL}$) groups respectively. Also, levels of HSP-70 were decreased with andrographolide treatment though not significantly (**Figure 2D, 2F**). Mean \pm SEM of densitometry for HSP-70 protein for control rats was found to be 0.29 \pm 0.02 while for LPS (2.5 $\mu\text{g}/\text{mL}$), Andrographolide (1 $\mu\text{g}/\text{mL}$) and LPS (2.5 $\mu\text{g}/\text{mL}$) along with andrographolide (1 $\mu\text{g}/\text{mL}$) groups were 0.44 \pm 0.13, 0.28 \pm 0.15, 0.17 \pm 0.04 respectively.

7.4. Suppression of NALP3 Inflammasome on Treatment with Andrographolide in IEC-6 Cells

Inflammasome pathway is popular in intestinal homeostasis (14). We found expression levels of NALP3 to decrease upon andrographolide treatment (**Figure 3A, 3B**). Mean \pm SEM of densitometry for NALP3 protein for control rats was found to be 0.65 ± 0.17 while for LPS (2.5 $\mu\text{g}/\text{mL}$), Andrographolide (1 $\mu\text{g}/\text{mL}$) and LPS (2.5 $\mu\text{g}/\text{mL}$) along with andrographolide (1 $\mu\text{g}/\text{mL}$) groups were 0.78 ± 0.12 , 0.37 ± 0.13 , 0.42 ± 0.08 respectively. The expression levels of Caspase-1, another important protein involved in NALP3 pathway, were also decreased in LPS-induced andrographolide cells (**Figure 3A, 3C**). Mean \pm SEM of densitometry for Caspase-1 protein were 1.08 ± 0.21 , 2.25 ± 0.57 , 0.92 ± 0.35 , 0.61 ± 0.30 in control, LPS (2.5 $\mu\text{g}/\text{mL}$), Andrographolide (1 $\mu\text{g}/\text{mL}$) and LPS (2.5 $\mu\text{g}/\text{mL}$) along with andrographolide (1 $\mu\text{g}/\text{mL}$) groups respectively.

7.5. Improvement in Pro-Inflammatory Cytokine Levels and Intestinal Villi on Treatment with Andrographolide

Hypobaric hypoxia upregulated the levels of pro-inflammatory cytokines i.e. TNF- α , IL-1 β , and IL-6 whereas the levels downregulated with the andrographolide treatment. Levels of TNF- α (**Figure 4A**) in control was 0.33 ± 0.01 pg/ml whereas andrographolide (20 mg/kg/BW), HH exposed and HH along with andrographolide (20 mg/kg/BW) groups had 0.34 ± 0.01 pg/ml, 0.45 ± 0.03 pg/ml and 0.37 ± 0.004 pg/ml respectively ($p < 0.01$ in control vs HH exposed and andrographolide vs HH exposed, $p < 0.05$ in HH exposed vs HH along with andrographolide). Rat IL-1 β levels were decreased significantly with andrographolide treatment ($p < 0.001$) (**Figure 4B**). Mean \pm SEM for IL-1 β levels in control was 0.05 ± 0.01 pg/ml, treatment groups had 0.12 ± 0.01 pg/ml, 0.40 ± 0.07 pg/ml and 0.09 ± 0.02 pg/ml in control, andrographolide (20 mg/kg/BW), HH exposed and HH along with andrographolide (20 mg/kg/BW) groups respectively. Levels of IL-6 (**Figure 4C**) in control was 0.26 ± 0.06 ng/ml whereas andrographolide (20 mg/kg/BW), HH exposed and HH along with andrographolide (20mg/kg/BW) groups had 0.22 ± 0.04 ng/ml, 1.42 ± 0.20 ng/ml and 0.63 ± 0.05 ng/ml respectively ($p < 0.001$ in control vs HH exposed and andrographolide vs HH exposed and $p < 0.01$ in HH exposed vs HH along with andrographolide). Jejunum tissue was stained with haematoxylin and eosin to observe

changes in intestinal villi. 7 days of hypobaric hypoxia has shown to cause loss in epithelial and goblet cell function, thus necrosis was observed in lumen of the intestinal villi. Andrographolide treatment was found to improve intestinal inflammation and necrosis as observed after 7 days of HH exposure (**Figure 4D**).

7.6. Effect of Andrographolide Treatment in HH Induced SD Rats

NALP3 inflammasome was suppressed by andrographolide treatment in SD rats. Levels of NALP3 (**Figure 5A, 5B**) and Caspase-1 protein (**Figure 5A, 5C**) were found to decrease with andrographolide treatment. Mean \pm SEM of densitometry for NALP3 protein were 0.49 ± 0.07 , 0.56 ± 0.12 , 1.29 ± 0.34 , 0.68 ± 0.34 ; while for Caspase-1 protein was 1.20 ± 0.26 , 1.16 ± 0.38 , 1.71 ± 0.36 , 1.43 ± 0.34 in control, andrographolide (20 mg/kg/BW), HH exposed and HH along with andrographolide (20 mg/kg/BW) groups respectively.

8. Discussion

Intestinal inflammation is common in IBD (Crohn's disease, ulcerative colitis), cancer and other types of infections [15]. There is no reliable treatment available in the market to cure these illnesses. In our study, we have seen the effect of andrographolide on *in vitro* and *in vivo* stress models. Previous research studies have reported that LPS results in intestinal inflammation when released and translocate across the intestinal barrier from gram-negative bacteria. Also in previous studies, hypobaric hypoxia has shown to affect intestine by causing inflammation and mucosal barrier injury [6, 16]. Studies have reported the translocation of endotoxins across the intestinal mucosal barrier initiates post mucosal barrier injury, thus making hypobaric hypoxia a good stress model to study the impact of andrographolide [17].

Inflammation is triggered upon damage detection by a set of receptors. NLRP3 being a broad sensor of cell homeostasis rupture is known for maintaining intestinal homeostasis and inhibiting inflammation caused by stressors [18, 19]. Also, NLRP3 inflammasome induces effects on the gut microbiome and modulates mucosal inflammation [20, 21]. NLRP3 inflammasome has various important effects on intestinal immune responses that result in the generation of IL-1 β . NLRP3 inflammasome plays a significant role in several inflammatory disorders including IBD [22].

Andrographolide is a major bio-constituent of *Andrographis paniculata*. It has shown some major pharmacological applications in Alzheimer's disease, cancer, arthritis, stroke, etc [23-26]. Studies have established its anti-inflammatory role in different diseases like asthma, etc [27]. In order to see the anti-inflammatory effect of andrographolide on the intestine, NLRP3 inflammasome pathway was studied in intestinal cells.

In our study, intestinal epithelial cells (IEC-6) were induced with LPS and andrographolide was given to circumvent the stress proteins thereby generated. Andrographolide has shown to reduce NO levels in LPS stimulated cells. Reduced NO levels were observed upon andrographolide treatment in previous studies in other type of cells e.g. macrophages [28,29]. Pro-inflammatory cytokines (TNF- α , IL-1 β , IL-6) were found to decrease with andrographolide treatment in both *in vitro* and *in vivo* studies. Results were similar to the study where pro-inflammatory cytokine levels reduced in colon tissues of experimental mouse colitis model with andrographolide treatment, highlighting the role of andrographolide as an anti-inflammatory drug [30].

Previous experimental studies have shown increased HSP-70 expression in colorectal mucosa of mice induced with colitis [31]. Therefore, it was mandatory to check the expression of HSPs in our gut inflammatory model. LPS induced intestinal epithelial cells have shown improvement in heat shock proteins expression (HSP-60 and HSP-70) with andrographolide treatment though not significantly. Also, NLRP3 inflammasome proteins have been downregulated with andrographolide treatment resulting in an improvement in intestinal homeostasis. Previous studies on colitis-associated cancer and IBD have also shown protection against intestinal inflammatory diseases by treatment of andrographolide via inhibition of NLRP3 pathway [32, 33].

The effect of andrographolide on intestinal problems like colon cancer, ulcerative colitis, etc., has been studied in many studies [30, 34, 35] but its role in circumventing the problems caused by HH has not been discovered yet. Our study involves andrographolide dosing to rats for 3 days and then exposing the animals to hypobaric hypoxia. Previous studies have shown proinflammatory cytokines to enhance HIF mediated gene expression with hypobaric hypoxia exposure [36]. Circumventing

pro-inflammatory cytokines could result in decrease in inflammation and similar results were observed in our study. Also, IHC images showed improved intestinal villi and epithelial and goblet cell function on the treatment of andrographolide. Similar improvements were also seen in DSS- induced colitis mice model [32]. The results correlate with the previous studies, where the NLRP3 pathway activates in response to any intestinal inflammation or injury to serve a protection from further loss [37, 38].

In conclusion, andrographolide may have a potential role in suppressing intestinal inflammation in LPS-induced and HH induced rats, thus could be a potential drug for the treatment of intestinal inflammation (**Figure 6**).

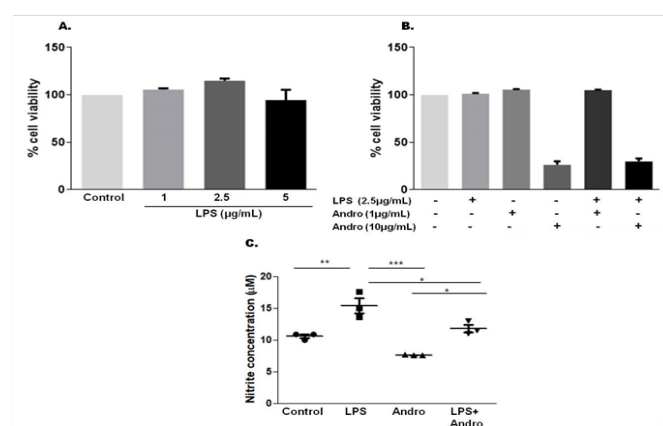


Figure 1: Cell viability and nitric oxide estimation in IEC-6 cells A. % cell viability estimation at different doses (1, 2.5 and 5 µg/mL) of LPS by MTT assay B. % cell viability estimation of cells at LPS alone 2.5 µg/mL, andrographolide alone (1 and 10 µg/mL) and combination of LPS and andrographolide by MTT assay C. Reduction of nitric oxide levels in LPS treated IEC-cells on treatment with andrographolide (1 µg/mL) (**p<0.05 in control vs LPS, ***p<0.01 LPS vs andrographolide and *p<0.05 LPS vs LPS plus andrographolide).

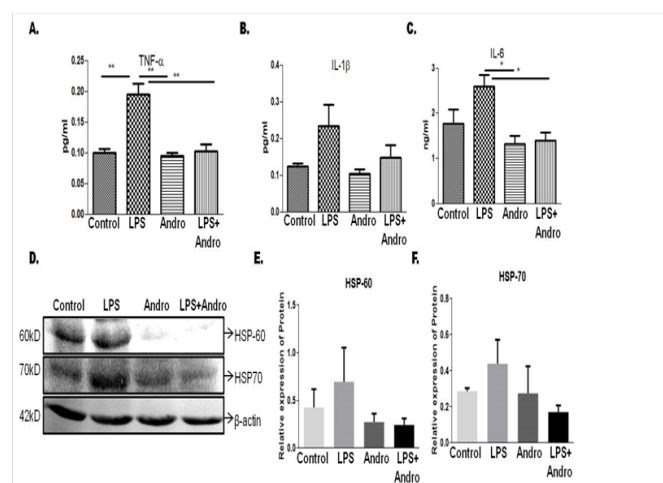


Figure 2: Estimation of levels of proinflammatory cytokines and expression of heat shock proteins A. Rat TNF- α levels in supernatant of control, LPS, andrographolide and LPS along with andrographolide groups (**p<0.01 in control vs LPS, LPS vs Andro and LPS vs LPS plus Andro) B. IL-1 β levels in cell supernatant of control vs treated groups C. IL-6 levels (*p<0.05 in LPS vs Andro and LPS vs LPS plus Andro) estimated in cell supernatant of control vs treated groups D. Blot image of heat shock proteins (HSP-60 and HSP-70) and loading control (β -actin) in. E. Quantification of expression of HSP-60 in all groups F. Quantification of expression of HSP-70 in all groups.

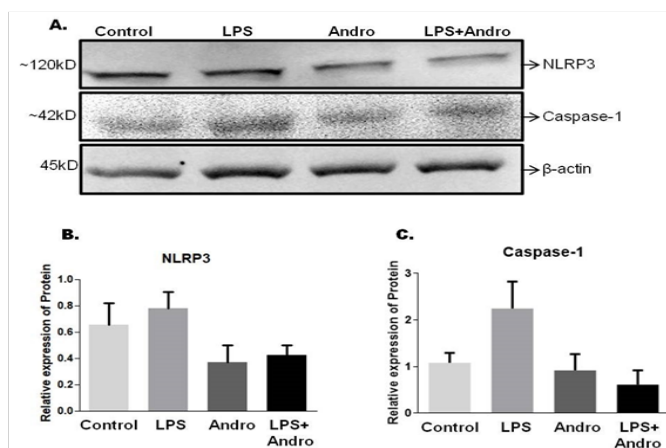


Figure 3: Analysis of NLRP3 and Caspase-1 in IEC-6 cells in control, LPS, andrographolide, and LPS plus andrographolide groups. A. Blot image of NLRP3, Caspase-1 and loading control (β -actin) in different groups. B. Quantification of expression of NLRP3 in all groups. C. Quantification of expression of caspase-1 to β -actin in all groups.

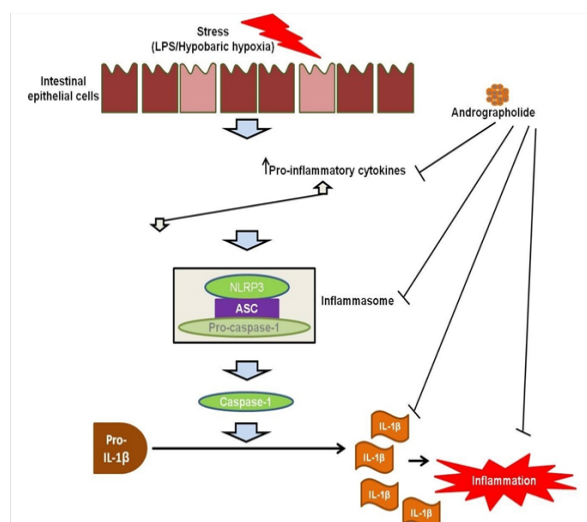


Figure 6: Summary of suppression of inflammation using andrographolide via NLRP3 pathway.

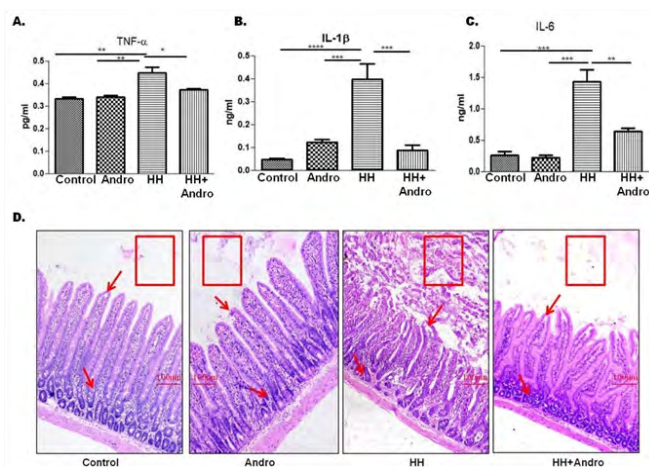


Figure 4: Levels of proinflammatory cytokines in gut lavage and H&E images of control and treated rats. A. Rat TNF- α levels in gut lavage of different groups (** $p < 0.01$ in control vs HH exposed and andrographolide vs HH exposed, * $p < 0.05$ in HH exposed vs HH along with andrographolide). B. Rat IL-1 β levels in control and treated cells (**** $p < 0.0001$ in control vs HH exposed and *** $p < 0.001$ in andrographolide vs HH exposed, *** $p < 0.001$ in HH exposed vs HH along with andrographolide). C. Rat IL-6 levels in gut lavage of different rat groups (*** $p < 0.001$ in control vs HH exposed and andrographolide vs HH exposed and ** $p < 0.01$ in HH exposed and HH along with andrographolide). D. H & E staining of jejunum tissue of control and treated rats. Results show improvement in intestinal inflammation and villi post andrographolide treatment.

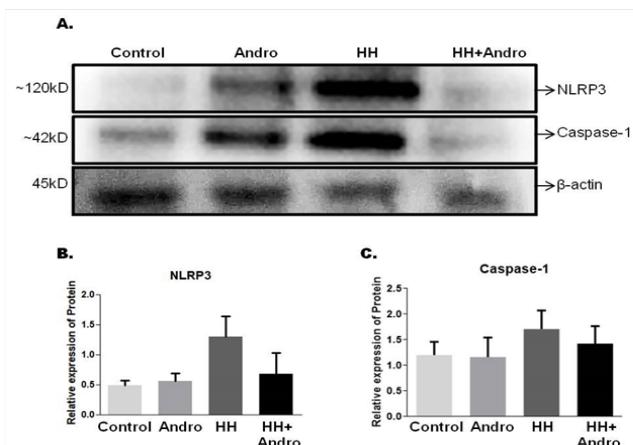


Figure 5: Analysis of NLRP3, Caspase-1 in jejunum tissue and IL-1 β in gut lavage of HH-exposed rats in control, andrographolide (20 mg/kg/BW), Hypobaric Hypoxia (HH) exposed (7 days) and HH plus andrographolide. A. Blot image of NLRP3, Caspase-1 and loading control (β -actin) in different groups. B. Quantification of expression of NLRP3 in all groups. C. Quantification of expression of caspase-1 to β -actin in all groups.

9. Acknowledgement

Authors thank Defence Research & Development Organization (DRDO), Ministry of Defence, Government of India, for financial support in the form of project DIP-265. KK thanks DRDO for providing fellowship in the form of junior and senior research fellowship.

References

- Kamboj VP. Herbal medicine. *Current Science*. 2000; 78: 35-9.
- Jayakumar T, Hsieh CY, Lee JJ, Sheu JR. Experimental and Clinical Pharmacology of *Andrographis paniculata* and Its Major Bioactive Phytoconstituent Andrographolide. *Evid Based Complement Alternat Med*. 2013; 2013: 846740.
- Cabrera D, Wree A, Povero D, Solís N, Hernandez A, Pizarro M et al. Andrographolide Ameliorates Inflammation and Fibrogenesis and Attenuates Inflammasome Activation in Experimental Non-Alcoholic Steatohepatitis. *Sci Rep*. 2017; 7: 3491.
- Tung YT, Chen HL, Tsai HC, Yang SH, Chang YC, Chen CM. Therapeutic Potential of Andrographolide Isolated from the Leaves of *Andrographis paniculata* for Treating Lung Adenocarcinomas. *Evid Based Complement Alternat Med*. 2013; 2013: 305898.
- Guo S, Al-Sadi R, Said HM, Ma TY. Lipopolysaccharide causes an increase in intestinal tight junction permeability in vitro and in vivo by inducing enterocyte membrane expression and localization of TLR-4 and CD14. *Am J Pathol*. 2013; 182(2): 375-87.
- Zhou QQ, Yang DZ, Luo YJ, Li SZ, Liu FY, Wang GS. Overstarvation aggravates intestinal injury and promotes bacterial

and endotoxin translocation under high-altitude hypoxic environment. *World J Gastroenterol.* 2011; 17: 1584-93.

7. Sharma JN, Al-Omran A, Parvathy SS. Role of nitric oxide in inflammatory diseases. *Inflammopharmacology.* 2007; 15: 252-9.

8. Gyires K, Tóth ÉV, Zádori SZ. Gut inflammation: current update on pathophysiology, molecular mechanism and pharmacological treatment modalities. *Curr Pharm Des.* 2014; 20: 1063-81.

9. He Y, Hara H, Núñez G. Mechanism and regulation of NLRP3 inflammasome activation. *Trends in biochemical sciences.* 2016; 41: 1012-21.

10. Gong Z, Zhou J, Li H, Gao Y, Xu C, Zhao S, et al. Curcumin suppresses NLRP3 inflammasome activation and protects against LPS-induced septic shock. *Mol Nutr Food Res.* 2015;59:2132-42.

11. Zhang P, Tsuchiya K, Kinoshita T, Kushiyama H, Suidasari S, Hatakeyama M, et al. Vitamin B6 Prevents IL-1 β Protein Production by Inhibiting NLRP3 Inflammasome Activation. *J Biol Chem.* 2016; 291:24517-27.

12. Li Z, Srivastava P. Heat-shock proteins. *Curr Protoc Immunol.* 2004; Appendix 1: Appendix 1T.

13. Habich C, Kempe K, van der Zee R, Rümenapf R, Akiyama H, Kolb H, et al. Heat shock protein 60: specific binding of lipopolysaccharide. *J Immunol.* 2005; 174:1298-305.

14. Gagliani N, Palm NW, de Zoete MR, Flavell RA. Inflammasomes and intestinal homeostasis: regulating and connecting infection, inflammation and the microbiota. *Int Immunol.* 2014;26:495-9.

15. Laroui H, Geem D, Xiao B, Viennois E, Rakhya P, Denning T, Merlin D. Targeting intestinal inflammation with CD98 siRNA/PEI-loaded nanoparticles. *Mol Ther.* 2014; 22:69-80.

16. Khanna K, Mishra KP, Chanda S, Eslavath MR, Ganju L, Kumar B, et al. Effects of Acute Exposure to Hypobaric Hypoxia on Mucosal Barrier Injury and the Gastrointestinal Immune Axis in Rats. *High Alt Med Biol.* 2018;20:35-44.

17. de Punder K, Pruijboom L. Stress induces endotoxemia and low-grade inflammation by increasing barrier permeability. *Front Immunol.* 2015;6:223.

18. Rathinam VAK, Chan FK. Inflammasome, Inflammation, and Tissue Homeostasis. *Trends Mol Med.* 2018;24:304-18.

19. Gros Lambert M, Py BF. Spotlight on the NLRP3 inflammasome pathway. *J Inflamm Res.* 2018;11:359-74.

20. Mao L, Kitani A, Strober W, Fuss IJ. The Role of NLRP3 and IL-1 β in the Pathogenesis of Inflammatory Bowel Disease. *Front Immunol.* 2018;9:2566.

21. Chen GY. Regulation of the gut microbiome by inflammasomes. *Free Radic Biol Med.* 2017;105: 35-40.

22. Nunes T, de Souza HS. Inflammasome in intestinal inflammation and cancer. *Mediators Inflamm.* 2013;2013:654963.

23. Geng J, Liu W, Xiong Y, Ding H, Jiang C, Yang X, et al. Andrographolide sulfonate improves Alzheimer-associated phenotypes and mitochondrial dysfunction in APP/PS1 transgenic mice. *Biomed Pharmacother.* 2018;97:1032-9.

24. Kandanur SGS, Nanduri S, Golakoti NR. Synthesis and biological evaluation of new C-12(α/β)-(N-) sulfamoyl-phenylamino-14-deoxy-andrographolide derivatives as potent anti-cancer agents. *Bioorg Med Chem Lett.* 2017;27(13): 2854-62.

25. Gupta S, Mishra KP, Singh SB, Ganju L. Inhibitory effects of andrographolide on activated macrophages and adjuvant-induced arthritis. *Inflammopharmacology.* 2018;26(2):447-56.

26. Yang CH, Yen TL, Hsu CY, Thomas PA, Sheu JR, Jayakumar T. Multi-Targeting Andrographolide, a Novel NF- κ B Inhibitor, as a Potential Therapeutic Agent for Stroke. *Int J Mol Sci.* 2017;18:E1638.

27. Abu-Ghefreh AA, Canatan H, Ezeamuzie CI. In vitro and in vivo anti-inflammatory effects of andrographolide. *Int Immunopharmacol.* 2009;9:313-8.

28. Chiou WF, Chen CF, Lin JJ. Mechanisms of suppression of inducible nitric oxide synthase (iNOS) expression in RAW 264.7 cells by andrographolide. *Br J Pharmacol.* 2000;129:1553-60.

29. Liu J, Wang ZT, Ji LL, Ge BX. Inhibitory effects of neoandrographolide on nitric oxide and prostaglandin E2 production in LPS-stimulated murine macrophage. *Mol Cell Biochem.* 2017;298:49-57.

30. Zhu Q, Zheng P, Chen X, Zhou F, He Q, Yang Y. Andrographolide presents therapeutic effect on ulcerative colitis through the inhibition of IL-23/IL-17 axis. *Am J Transl Res.* 2018;10:465-73.

31. Samborski P, Grzymisławski M. The Role of HSP70 Heat Shock Proteins in the Pathogenesis and Treatment of

Inflammatory Bowel Diseases. *AdvClinExp Med.* 2015;24:525-30.

32. Guo W, Sun Y, Liu W, Wu X, Guo L, Cai P, et al. Small molecule-driven mitophagy-mediated NLRP3 inflammasome inhibition is responsible for the prevention of colitis-associated cancer. *Autophagy.* 2014;10:972-85.

33. Ke P, Shao BZ, Xu ZQ, Chen XW, Liu C. Intestinal Autophagy and Its Pharmacological Control in Inflammatory Bowel Disease. *Front Immunol.* 2017;7:695.

34. Zhang R, Zhao J, Xu J, Jiao DX, Wang J, Gong ZQ, et al. Andrographolide suppresses proliferation of human colon cancer SW620 cells through the TLR4/NF- κ B/MMP-9 signaling pathway. *Oncol Lett.* 2017;14:4305-10.

35. Liu W, Guo W, Guo L, Gu Y, Cai P, Xie N, et al. Andrographolide sulfonate ameliorates experimental colitis in mice by inhibiting Th1/Th17 response. *IntImmunopharmacol.* 2014; 20:337-45.

36. Liu X, He L, Dinger B, Stensaas L, Fidone, S. Sustained exposure to cytokines and hypoxia enhances excitability of oxygen-sensitive type I cells in rat carotid body: correlation with the expression of HIF-1 α protein and adrenomedullin. *High altitude medicine & biology.* 2013;14:53–60.

37. Song-Zhao GX, Srinivasan N, Pott J, Baban D, Frankel G, Maloy KJ. Nlrp3 activation in the intestinal epithelium protects against a mucosal pathogen. *Mucosal Immunol.* 2014;7:763-74.

38. Alhallaf R, Agha Z, Miller CM, Robertson AAB, Sotillo J, Croese J, et al. The NLRP3 Inflammasome suppresses Protective Immunity to Gastrointestinal Helminth Infection. *Cell Rep.* 2018;23:1085-98.